An experimental and signal analysis workflow for detecting cold-induced noise emissions (cold squealing) from porous journal bearings

S. J. Eder[a,*], D. Bianchi[a], I. A. Neacşu[a], G. Vorlaufer[a]

[a] *AC2T research GmbH, Viktor-Kaplan-Straße 2, 2700 Wiener Neustadt, Austria*

Abstract

We employ a variant of the joint time-frequency analysis (JTFA) for identifying transient, temperature-dependent noise emitted from porous journal bearings operated at temperatures between –40°C and 0°C. This phenomenon, called "cold squealing", is difficult to reproduce in laboratory environments, as it requires a suitable (and typically system-specific) resonator to occur. We systematically tested real-world bearings impregnated with various oils on a custom-designed experimental rig, fitted with a coolable sample holder and a vibration sensor, over a range of rotational speeds. By analyzing temperature-differential JTFA signal maps, we succeeded in detecting transient cold-squealing as well as ranking the bearing lubricants according to their low-temperature quiet running properties.

Keywords: joint time-frequency analysis, porous journal bearings, tribology, cold squealing

1. Introduction

In the automotive industry, components such as brakes as well as bearings used in windshield wipers, power window lifts, fans, and air conditioners can emit unpleasant noises under certain operating conditions, which usually leads to customer complaints or even product recalls.

A journal bearing is a simple and cheap mass-production machine element, which operates paired with a matching shaft of a drive. Porous journal bearings are produced from metal powders by sintering, and their resulting porous structure is later impregnated with a lubricant like a sponge [1, 2]. The permanent oil circulation between the bearing's porous seat and the lubrication gap gives them the advantage of "life-time lubrication", i.e., they are functional for their entire service life of typically 3000 to 10 000 hours [3, 4]. Due to their flexibility in design and maintenance-free operation, they are very often used in industrial applications where an external supply of oil is not possible. Providers of automobile parts wish for smoothly running bearings, in particular the prevention of so-called "cold squealing" at temperatures below –20°C, so choosing the right combination between bearing material and lubricant is crucial. On the other hand, the full functionality and the service life of the bearing in the temperature range from –40°C to +120°C must be kept, since operation has to remain possible in cold regions as well as in the hot engine compartment [5, 6]. References [2, 7] reported the occurrence of noise in porous journal bearings when certain types of lubricants are used, but their tests focused on high-temperature operation only. Numerous lubricants have frequently failed in terms of quiet operation, especially at low temperatures.

The motivation for this work stems from an automobile parts manufacturer commissioning one of its lubricant providers to formulate a new porous bearing lubricant to fulfill a set of requirements including the ones mentioned above. Out of the handful of novel laboratory formulations, some were already discarded in-house by the lubricant manufacturer due to inadequate evaporation and/or static oil aging results. One more candidate formulation had to be discarded due to poor tribological performance at high temperature. Therefore, two new formulations remained that had to be tested for the most beneficial low-temperature properties.

While there is some literature available on brake squeal and ways to reduce it [8, 9, 10], cold start squealing of clutches [11] or engines [12], as well as more general work on friction-induced vibration, chatter, and squeal [13], the phenomenon of cold squealing bearings is relatively unstudied. Annoying as the latter may be, it is relatively difficult to consistently reproduce it in laboratory experiments, which impairs the studying of its origins.

It is generally understood that cold squealing is a friction-induced resonance phenomenon in the sense that a positive feedback between rapidly changing friction forces in the bearing and vibrational motion of the shaft may excite eigenmodes of the surrounding components, which in turn are emitted as airborne sound waves with sufficient acoustic pressure [14]. The origin of the rapid change in friction conditions is caused by a sudden transition from boundary or mixed to hydrodynamic lubrication, e.g., because of a cold, highly viscous bearing lubricant.

*Corresponding author
Email address: stefan.eder@ac2t.at (S. J. Eder)

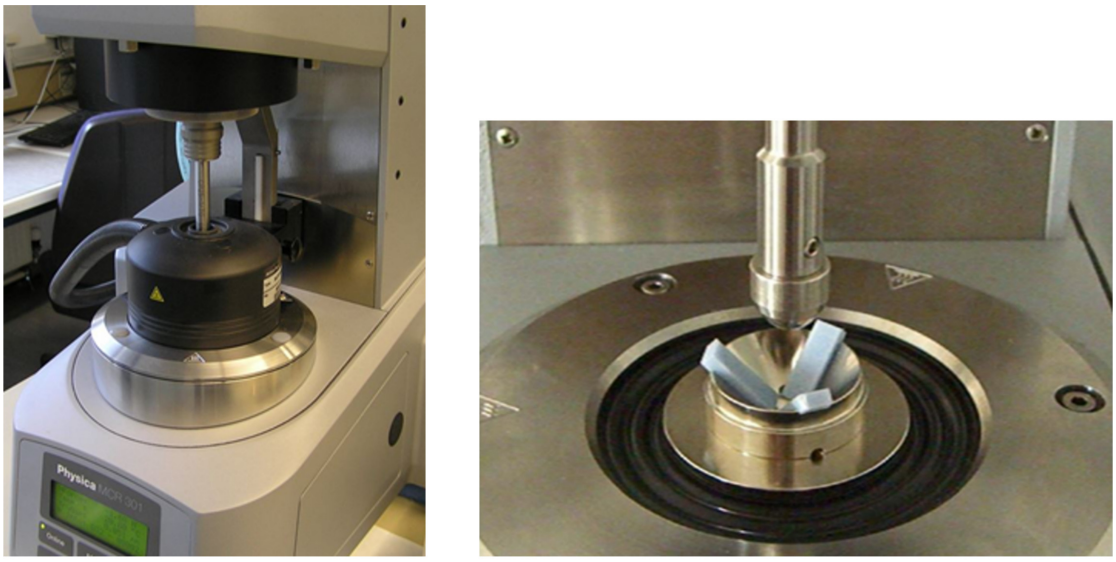

(a) (b)

Figure 1: The Physica MCR 301 rheometer by Anton Paar. (a) In operation with Peltier cap. (b) The ball-on-plate geometry of the tribocell with three blocks of plastic in the positions where the porous plates are held in place by a clip (not shown) during testing.

Most tribometers available for testing the performance of porous bearings are relatively stiff and do not feature an appropriate resonator, which means that the measuring and analysis approach must be able to detect transient or even inaudible noise emissions. In this work we will present such an approach based on the measurement of structure-borne noise as well as methods borrowed from voice analysis. We will exemplify our approach by ranking five porous bearing lubricants according to their cold-noise performance, which eventually led to the commercialization of the best-performing lubricant.

2. Model Tribometers and Experimental Procedure

In this section we will introduce the two test devices that we used to experimentally reproduce the cold squealing phenomenon. The first one, a rheometer, was chosen because it allows isothermal testing, so that the point at which cold squealing occurs can be located via manual tweaking of the rotational speed. The second one, a custom-designed tribometer, performs rotational speed ramps after an initial cooling, so that the temperature varies due to the friction energy dissipation in the bearing.

Preliminary studies were carried out on a stress-controlled rotational rheometer with air bearings, the Physica MCR 301 by Anton Paar, see Fig. 1 (a). The tribocell constituting its core is a ball-on-plate model system. The ball (diameter 12.7 mm) is pressed against three plates with an angle of 45° to the vertical axis and 120° between each other, thus creating three point contacts, see Fig. 1 (b). While the ball rotates or oscillates, the torque and normal forces are recorded. The temperature can be regulated with Peltier elements positioned in the cap and the bottom. This setup offers a temperature range of –40°C to +200°C at a precision better than 0.1°C. Reaching –40°C from room temperature can be achieved in approximately 10 minutes. The rotating speed can be adjusted between 10^{-7} and 3000 min^{-1}, the torque measurement resolution is 0.001 Nmm, and test procedures are fully programmable. The tribocell is suitable for static friction measurements, the generation of Stribeck-curves, and friction measurements with axial guidance. As the three porous plates constituting the base body are spring-mounted, the occurring operational system oscillations are provided with a resonator, which facilitates the reproduction of cold-induced squealing. However, as the system geometry is completely different from a loaded bearing with a shaft, the transferability of any results to real systems is highly limited.

The initial feasibility tests to ascertain the general reproducibility of cold-induced operation noises were performed on the Physica MCR 301. Due to the transferability issue mentioned above, these tests do not follow a strict procedure and merely serve as a source of examples to be analyzed using the workflow described in Sect. 3. They were carried out by placing three plates made from porous bearing material, soaked in a test lubricant, in the tribocell as shown in Fig. 1 (b). After installation of the cryo-cap, the system was cooled down using the Peltier elements. When the operating temperature of –40°C was reached, the ball was pressed against the plates at a small load to facilitate the formation of oscillations. The rotational speed was then manually adjusted, maintaining –40°C, until cold squealing occurred, and the sound emissions were recorded using a microphone.

In an effort to reproduce cold squealing emitted by tribosystems consisting of real porous journal bearings and

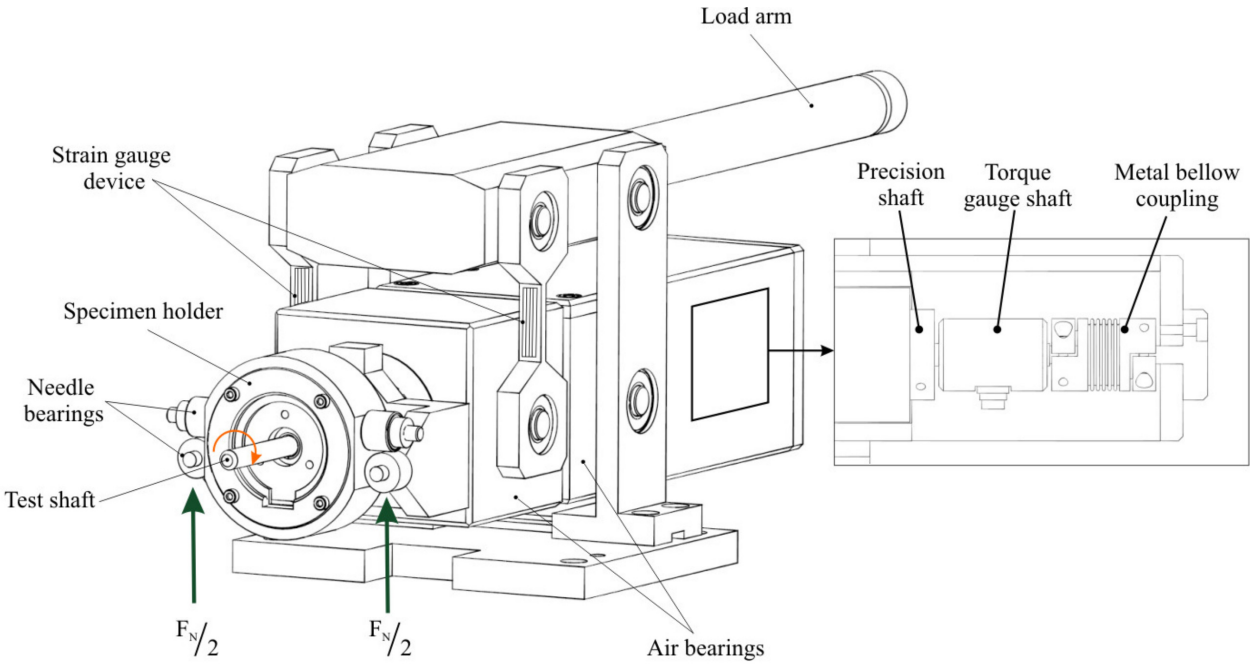

(a)

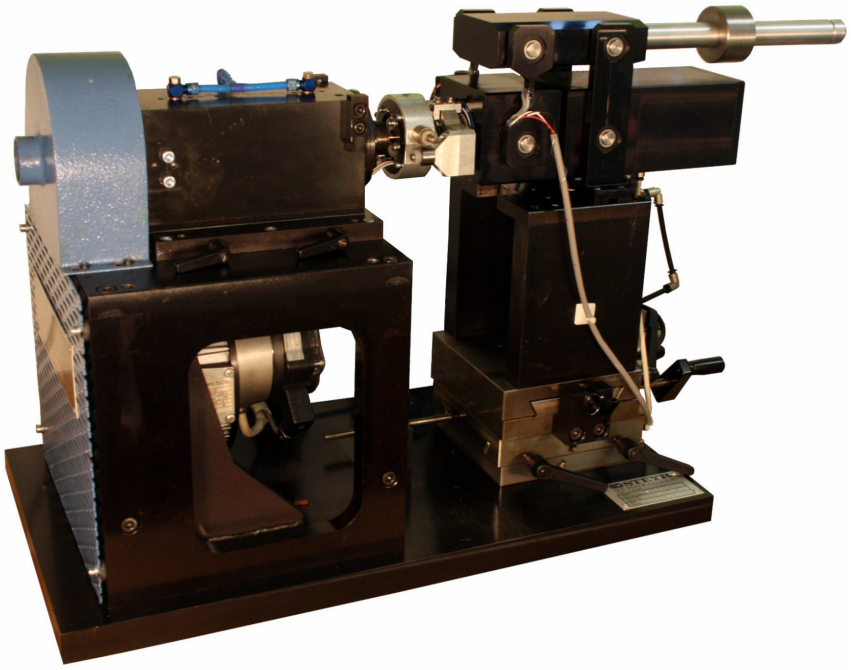

(b)

Figure 2: Experimental test rig SLPG2. (a) Annotated sketch, (b) Real image of the entire setup including drive.

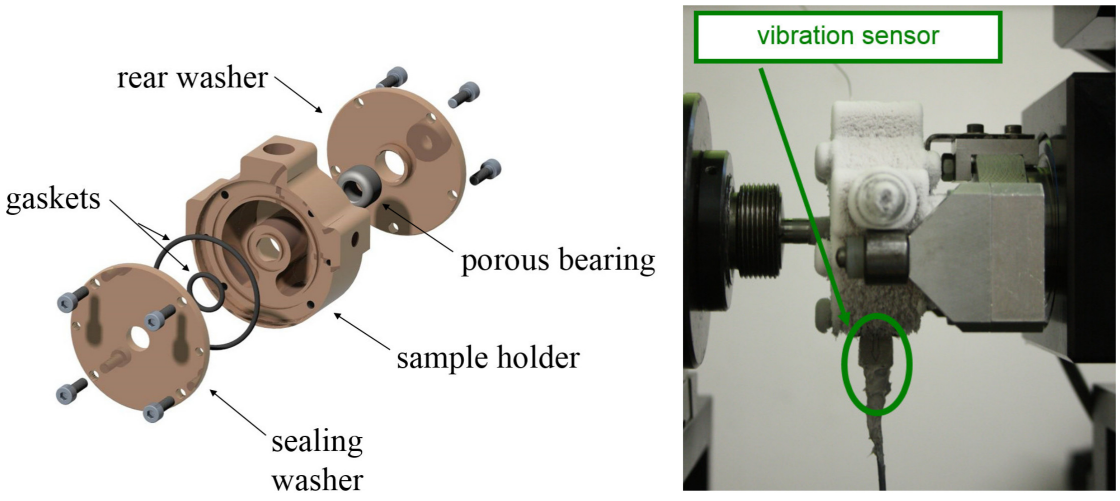

(a) (b)

Figure 3: Sketch of the coolable sample holder for the SLPG2 test rig (a). Side view of the sample holder in action (frozen over) with the vibration sensor attached to its base.

shafts, we experimented with spherical bearings of 11 mm length and 8.01 mm bore diameter made from sintered steel with 2% copper and a porosity of 20%. These "standard bearings" were paired with 8 mm hardened steel shafts, and the experiments were performed on a custom-made test rig for precision bearings, named "SLPG2" (from the German "Sinterlagerprüfgerät 2", "porous bearing test device, version 2"), as described in more detail in [15]. Its specific design, see Fig. 2, allows the programming of a multitude of test procedures and the automatic recording and analysis of the test temperature, the shaft rotational speed, the normal load, and the friction torque. With the aid of a chuck, a shaft can be (interchangeably) installed on a spindle mounted with precision roller bearings (max. concentricity deviation of 2 μm, rotational speed up to 18 000 min^{-1}). The free end of the shaft (typical diameter range 4–12 mm) is fitted with the test bearing in a holder. A torsion measurement device based on essentially frictionless air bearings integrated into the loading mechanism allows the measurement of the friction torque in the test bearing. The maximum allowed radial loading is 200 N. The bearing holder can be fitted to the bearing externally, independent of the test device, and prepared for the test run. It is compatible with numerous bearing dimensions and geometries via a set of adapters that allow simple assembly of the bearing–shaft pairing as well as installation in the test device. Variants of the mount provide initial cooling, output-regulated heating, temperature measurement, and monitoring of the lubrication conditions.

For the cryo-experiments, a coolable sample holder was constructed for the SLPG2. It features a copper cooling element that can be brought to the desired temperature by filling it with an appropriate coolant, see Fig. 3 (a). In our experiments, we used liquid nitrogen as a coolant, inserted into the top hole via a paper funnel. Using a plastic clip, a piezo-electrical vibration sensor with an effective measuring range from 0.5 Hz to 2 kHz and a sampling rate of 10 kS/s was fixed to the base of the sample holder. The sensor measures the out-of-plane oscillation of the surface to detect bearing vibrations. In order not to severely degrade the vibration signal quality, it is important to ensure that all effervescence of the evaporating nitrogen has ended before an experiment starts. This implies that a replenishment of the coolant is no longer possible once the measurement has started.

The experimental procedure for the cryo-experiments on the SLPG2 was somewhat more elaborate than that for the preliminary tests in the Physica MCR 301 in order to test only run-in tribosystems and to ensure maximum comparability between tests:

- Running-in for 16 h at a normal load of 100 N and room temperature. During this procedure, the rotational speed of the shaft is repeatedly linearly ramped from 0–3000–0 min^{-1} with a period of 6 min, which allows the constant diagnostic recording of Stribeck curves. By monitoring the coefficients of friction at 0 min^{-1} and 3000 min^{-1} as well as the friction minimum for each curve, it becomes apparent when the bearing and the shaft have run in, see Fig. 4.
- Initial cooling of the sample holder with liquid nitrogen
- Automatic starting of the tribometer motor when $T_{target} = -40°\mathrm{C}$ is reached
- Repeated rotational speed ramps until $T = +10°\mathrm{C}$. Depending on the system, this ranges from three to six ramps.
- Perform cooled experiments at 200 N, 100 N, 50 N, and 10 N.

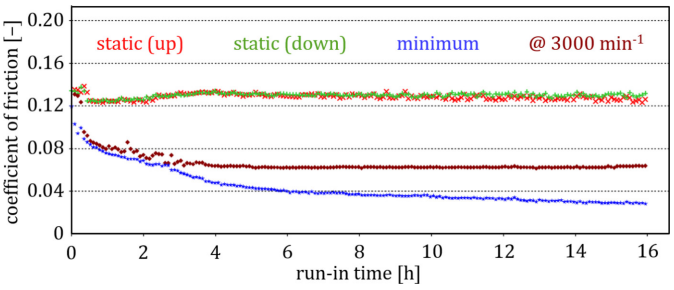

Figure 4: Monitoring the running-in process, in this example for lab sample Lab-2. Every column of data points represents four points evaluated from a Stribeck curve at 100 N and room temperature: the static coefficients of friction at the beginning and the end of the speed ramp, the friction minimum, and the coefficient of friction at the maximum rotational speed.

3. Analysis Method for Evaluating Bearing Vibrations

As mentioned earlier, porous journal bearings may exhibit friction instabilities caused, for example, by repeated transitions from mixed to hydrodynamic lubrication conditions [16]. These instabilities cause transient vibrations, which in turn are detected by a piezo-electric vibration sensor attached to the body of the sample holder, and recorded as acceleration values in units of the gravitational acceleration, g. In order to capture the transient nature as well as the characteristic spectrum of the vibrations, the vibration sensor signal is analyzed using a variant of the so-called *joint time-frequency analysis* (JTFA) [17, 18], a technology with applications such as voice analysis and identification. In this analysis, the recorded signal is first multiplied by a moving window function and subsequently transformed into Fourier space using the fast Fourier transform. Formally the JTFA is related to the short-time Fourier transform of a time continuous signal, given by

$$\hat{u}(t,f) = \int_{-\infty}^{\infty} u(t-\tau)w(\tau)\exp\left[-2\pi j f\tau\right]d\tau \ , \qquad (1)$$

see Ref. [19]. Here, t and f denote time and frequency, respectively, and $u(t)$ and $\hat{u}(t,f)$ represent the time signal and its short-time Fourier transform. $w(t)$ is a windowing (weighting) function localized both in the time and frequency domain. It has to be noted that due to the Heisenberg uncertainty principle [20], a signal cannot be arbitrarily localized in both time and frequency.

In the case of time-discrete signals, sampled with sampling rate s, i.e.,

$$u_i = u(t_i) = u(i\Delta t), i \in N_0 \ , \qquad (2)$$

where $\Delta t = 1/s$ is the time interval between two consecutive sampling time stamps, a discretized window function with finite support may be defined as

$$w_k = w(k\Delta t), \quad k = 0 \ldots K-1 \ . \qquad (3)$$

Then, equation (1) may be approximated by

$$\hat{u}_{l,m} = \hat{u}\left(l\Delta t, m\Delta f\right) \approx \Delta t \sum_{k=0}^{K-1} u_{l-k} w_k \exp\left[-2\pi j \frac{km}{K}\right] . \qquad (4)$$

Equation (4) is the basis for the JTFA, which is exactly the length K discrete Fourier transform of the sequence $\langle u_l w_0, u_{l-1} w_1, \ldots, u_{l-K+1} w_{K-1}\rangle$. The frequency resolution Δf is given by

$$\Delta f = \frac{s}{K} \qquad (5)$$

In our case, the sample rate s is set to 10 kHz and $w(t)$ is a cosine window with a width of 400 ms, i.e., $K = 4000$, Thus, the frequency resolution is 2.5 Hz.

Typically, the result of the JTFA is visualized as a heat map with time and frequency as the horizontal and vertical axes, respectively, and the amplitude $|\hat{u}_{l,m}|$ coded in color. These maps provide an excellent visual overview of the measured vibrations, see the visualizations of the preliminary isothermal experiments, carried out at constant rotational speed, with the Physica MCR 301 rheometer in Fig. 5. These three examples, in which an experienced

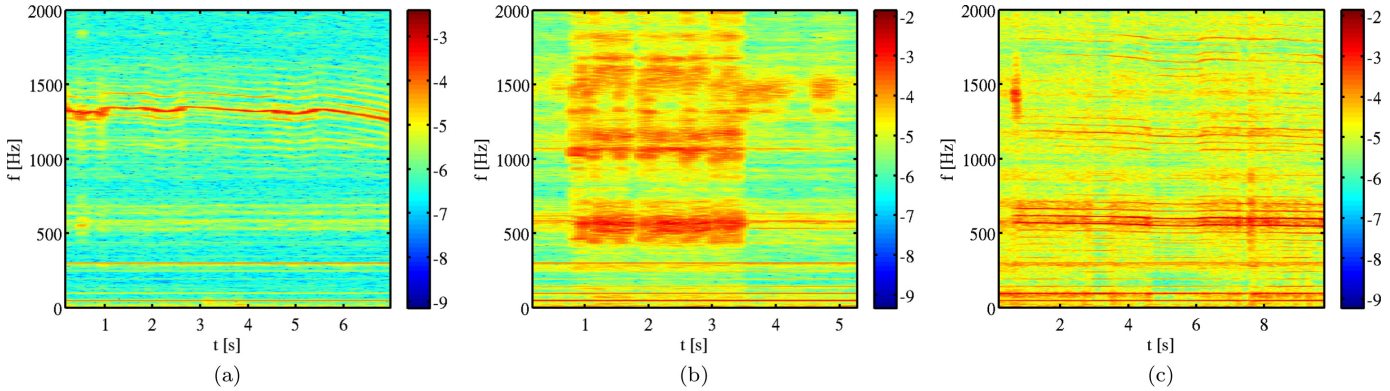

Figure 5: JTFA signal maps obtained from sound recordings of cold squealing reproduced in the Physica MCR 301 rheometer. (a) "singing" at approximately 1300 Hz, (b) "whinnying" with overlayed "chirping", and (c) "trilling drone".

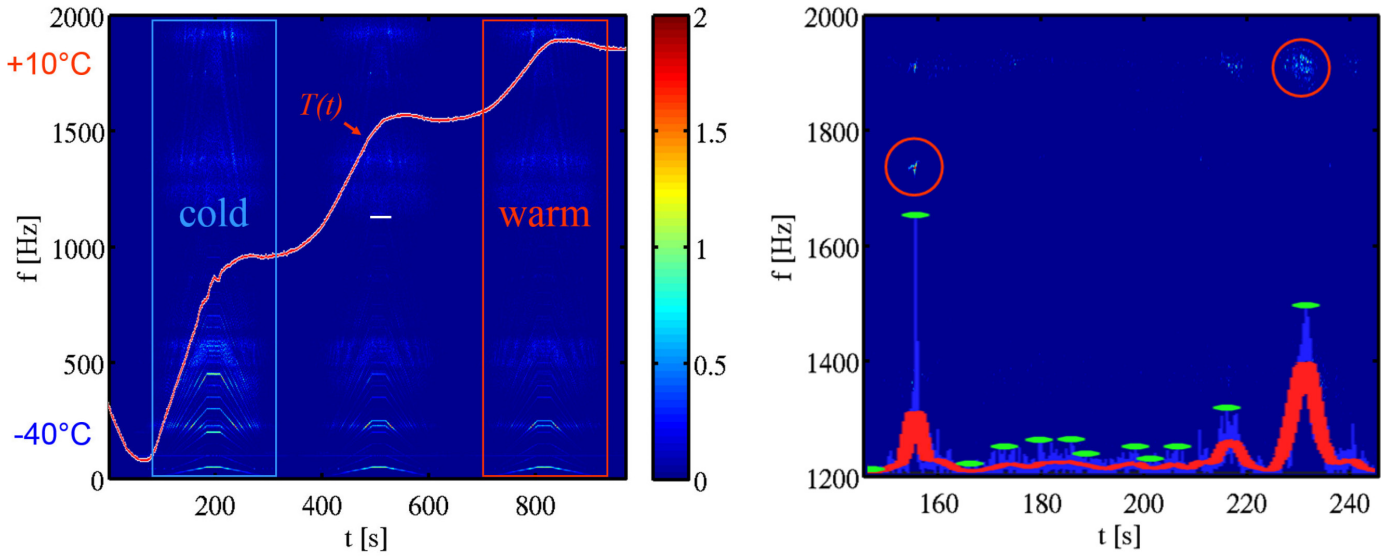

Figure 6: (a) JTFA signal map of the vibration signal during a cryo-experiment on the SLPG2 tribometer with Ref-V68, temperature profile superimposed. The colors of the map indicate the vibration acceleration amplitude at the respective time in the corresponding frequency range (in multiples of g). (b) Representation of the filtered amplitude difference between warm and cold operation. The special events (temperature-dependent sound emissions) are marked with red circles and a smoothed total sound intensity is superimposed as a red curve (arbitrary units).

engineer ascertained that the analyzed signals in fact correspond to cold squealing, give an impression of which sort of patterns to look out for when analyzing vibration data from real systems. In contrast to a global frequency spectrum, the JTFA signal maps also allow the identification of transient noises occurring only for brief periods, see the visualization of a cryo-experiment conducted with the SLPG2 tribometer in Fig. 6 (a).

A semi-automatic routine for recognizing temperature-dependent noise emissions facilitates the identification of the thermally relevant frequency bands. This allows the first experiment to be evaluated during the first follow-up trial, so that the second follow-up trial may already be adapted, if necessary. The routine is "semi-automatic", because the user can vary several parameters that, depending on the actual data, can increase the quality of the obtained results. The *time resolution* of the JTFA effectively sets the ratio between the resolutions on the time and the frequency axes (in seconds). The *high-frequency window* sets the range in which to search for temperature-dependent squeals (in Hz). The *noise threshold* determines up to which acceleration the signal is considered random noise (in multiples of g). Finally, the *smoothing window width* reflects the strength with which the high-frequency signal is smoothed using a Gaussian filter in order to locate the relevant peaks (in seconds). In our workflow, we obtained the best results with values for these parameters of 0.2 s, 1200–2000 Hz, 0.2 g, and 4 s, respectively.

By calculating a filtered amplitude difference $\Delta A(f,t)$ between a "cold" and a "warm" measurement (see Fig. 6 (b)), we can identify those noise contributions that differ due to the temperature, see Fig. 6 (b). A simple summation over the noise amplitudes allows the calculation of the points in time when the most prominent differences occur, see the superimposed spectrum in Fig. 6 (b). A comparison of the cold and warm spectra around these points shows which regions of the spectrum are affected most by the temperature difference (Fig. 7).

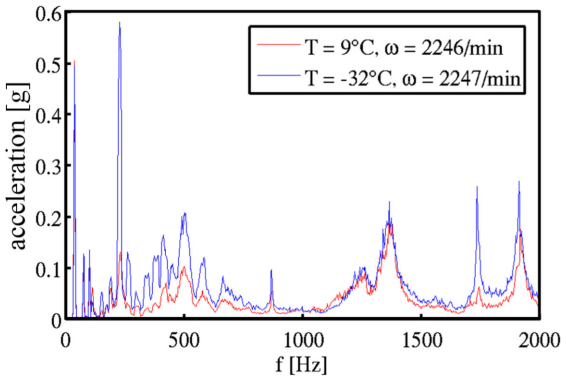

Figure 7: Comparison of a cold (blue) and a warm (red) frequency spectrum for Ref-V68. Many frequencies below 800 Hz associated with the motor are greatly damped at higher temperatures, and a sharp peak at 1750 Hz is also strongly temperature dependent.

We identified the critical rotational speeds of the SLPG2 tribometer using standard industry shafts with orbiform cross-sections and the PAO-based porous bearing oil Ref-V68, as this oil was deemed likely to produce cold squealing due to its relatively high viscosity of 68 mm^2/s at 40°C,

Table 1: PAO-based porous bearing lubricants and their viscosities at 40°C, tested for low-temperature quiet running properties.

ID	V@40°C [mm^2/s]	note
Ref-V68	68	benchmark reference
Ref-V100	100	additional benchmark
Lab-1	18	new formulation with thickener
Lab-2	18	new formulation without thickener
Lab-3	46	unadditivated, non-competitive

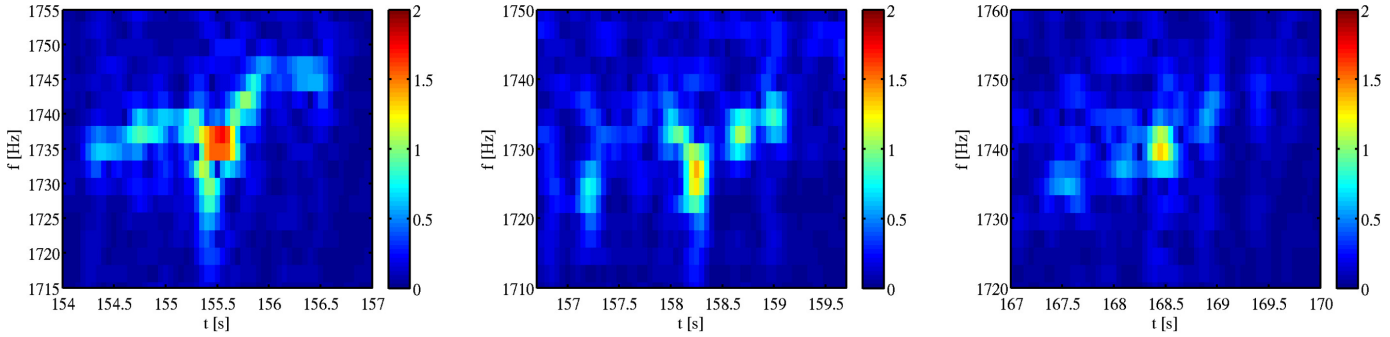

Figure 8: Illustrative JTFA signal map close-ups of the most prominent cold-induced sound emission occurring at $L = 100$ N between 1700 and 1750 Hz. (a) Ref-V68, (b) lab sample Lab-1, (c) lab sample Lab-2.

cf. Table 1. The most obvious instances of cold-induced noises, namely a "singing" sound of approximately 1750 Hz at a rotational speed of 2250 min^{-1} and a more diffuse noise of about 1900 Hz at 2400 min^{-1} were compared to the oils Lab-1 and Lab-2, see Fig. 8, both of which were custom formulated for excellent low-temperature performance, as well as to an unadditivated PAO base oil with the sample code Lab-3. To this end, we averaged the squared vibration amplitude, which is proportional to the vibration intensity, over the frequency band and the time window relevant for the noise and plotted that quantity over the average temperature for the respective time window. Figure 9 shows the comparison between the four oils for the two chosen temperature-dependent noises.

At the lowest temperatures between –30°C and –40°C, both newly formulated oils exhibit much less sound emission than the Ref-V68, although the latter becomes considerably less noisy at temperatures exceeding 0°C. Here, the vibration intensities drop by roughly one order of magnitude compared with the low-temperature values. We note the high noise emissions obtained with the oil Lab-1 at the critical rotation speed of 2400 min^{-1} around 0°C, which may indicate the presence of residual water in the system.

4. Temperature Dependence of Bearing Noise Development

In addition to the cold squealing comparison, we ranked the noise emissions of five lubricants in standard bearings against standard shafts, differentiated by frequency range and rotational speed. For an overview of all five ranked lubricants, see Table 1.

As before, cryo-experiments were carried out at a load of 100 N and started at a temperature of –40°C. The rotational speed ramps from 0–3000 min^{-1} were repeated until the system temperature had risen above +10°C. Every experiment was repeated once. The vibration intensities obtained via the JTFA were averaged over blocks defined by two frequency bands (0–1000 Hz, 1000–2000 Hz) and three rotational speed ranges (0–1000 min^{-1}, 1000–2000 min^{-1}, 2000–3000 min^{-1}). At the same time, we evaluated the average temperature and friction torque for each of these blocks, allowing us to compare vibration emissions and friction performance as a function of temperature. Figure 10 summarizes several of the results that we will discuss in the following.

Ref-V68 and especially Ref-V100 have a tendency towards startup noise, i.e., high vibrational intensities in the lower frequency band (0–1000 Hz) and at low rotational speeds (0–1000 min^{-1}). Otherwise, all five tested lubricants perform similarly well in this frequency and rotational speed block, independent of temperature. In the middle rotational speed range 1000–2000 min^{-1}, the lower frequency band shows incipient separation of the data for the fully formulated reference oils (more noise) from that of the other tested oils (less noise). At the highest rotational speeds (2000–3000 min^{-1}), Ref-V100 is markedly louder warmed up (by a factor of $\simeq 2.5$) than the other oils are cold, Ref-V68 is slightly louder than the lab samples and exhibits a higher temperature gradient. Lab sample Lab-2

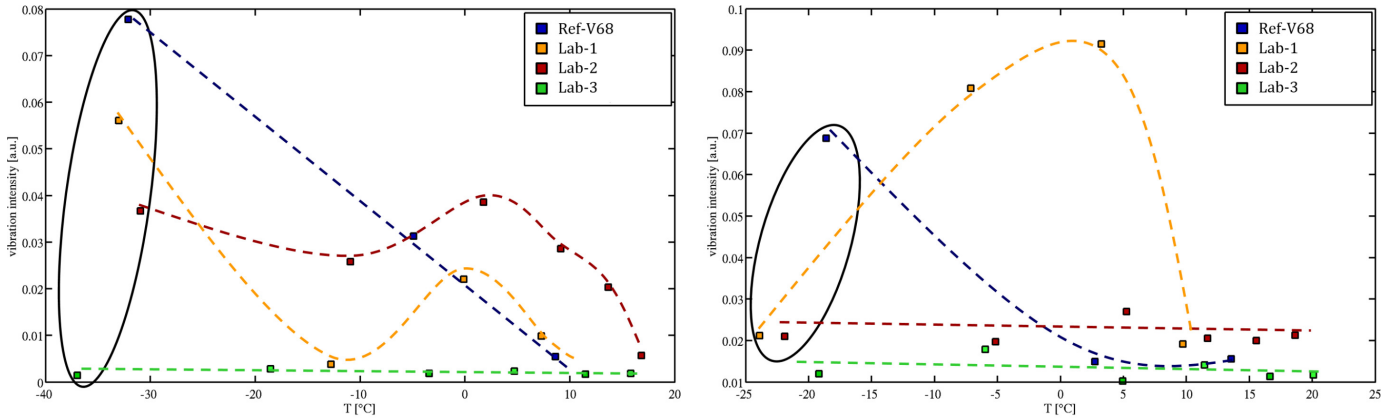

Figure 9: Comparison of the temperature dependence of the two critical sound emission windows for cold squealing around 1750 Hz, 2250 min^{-1} (a) and 1900 Hz, 2400 min^{-1} (b).

produces slightly less noise in the second experiment than in the first, see Fig. 10 (e–f).

In the upper frequency band (1000–2000 Hz), the system lubricated with Ref-V68 is the noisiest at low temperatures, independent of rotational speed, but emissions drop below those obtained with Lab-1 for $T > -5°\mathrm{C}$. Ref-V100 runs quietly at low rotational speeds, but becomes overproportionally louder at higher rotational speeds. The unadditivated PAO lab sample Lab-3 produces the lowest noise emissions, except for low temperatures and low rotational speeds. Lab sample Lab-1 is louder than Lab-2 at all temperatures, with the differences being greatest for $T > 0°\mathrm{C}$.

The matrix in Fig. 11 gives a summary of the ranking, comparing the oils in various aspects of their cold running properties, where beneficial behavior is marked by a green field, poor behavior by a red one, and average by yellow. Note that the ranking was carried out subjectively, based on the available data, as well as relative for every category, i.e., even if all lubricants had behaved similarly, the poorest one would have been ranked "red" in that category. Of the two newly formulated oils, lab sample Lab-2 exhibits the best overall performance. It should be noted that the unadditivated lab sample Lab-3 performs surprisingly well with respect to cold properties, but in order to be better comparable with the rest of the contenders, it would be necessary to test the fully additivated version as well. From this, it might be deduced that the original requirement for the newly formulated lubricant to have a base oil viscosity of no more than 18 mm^2/s, which was stipulated with low-temperature properties in mind, may not have been as stringent. It might also be a hint that the standard additivation plays an important part in the deterioration of cold-running performance.

5. Summary and Conclusion

The presented measurement assembly and analysis approach allow the quantification of the SLPG2 tribometer's tendency to vibrate under a given set of circumstances. By working through a test matrix with various porous bearing lubrication oils, we could investigate the influence that these oils have on the vibrations. Using our custom-made semi-automatic noise detection and comparison software including an implementation of the joint time-frequency analysis, we can identify cold-induced noises of limited duration. This allows us to pinpoint the rotational speeds critical for the test system, where cold-induced noises can occur, and to compare noise emissions of systems lubricated with different oils at these rotational speeds. The most distinct squealing sounds could be produced using the shafts with orbiform cross-sections at a load of 100 N. However, even with more round shafts that do not produce any obvious squealing noises, it is possible to produce a low-temperature noise ranking differentiated by rotational speed range and frequency band. The categorization of the cold running properties allows a ranking of the tested lubricants, among which the newly formulated oil Lab-2 exhibited the most beneficial overall performance. This eventually led to the commercialization of the product.

Acknowledgment

This work was funded by the Austrian COMET-Program (Project K2, XTribology, no. 849109) and carried out at the "Excellence Centre of Tribology". Thanks to Erwin Mayrhofer for setting up the test rig with the vibration sensor and Christoph Haslehner for performing the experiments.

References

[1] VT Morgan and A Cameron. Mechanism of lubrication in porous metal bearings. *Proceeding conference on Lubrication and Wear*, pages 151–175, 1957.

[2] AL Braun. Porous bearings. *Tribology international*, 15(5):235–242, 1982.

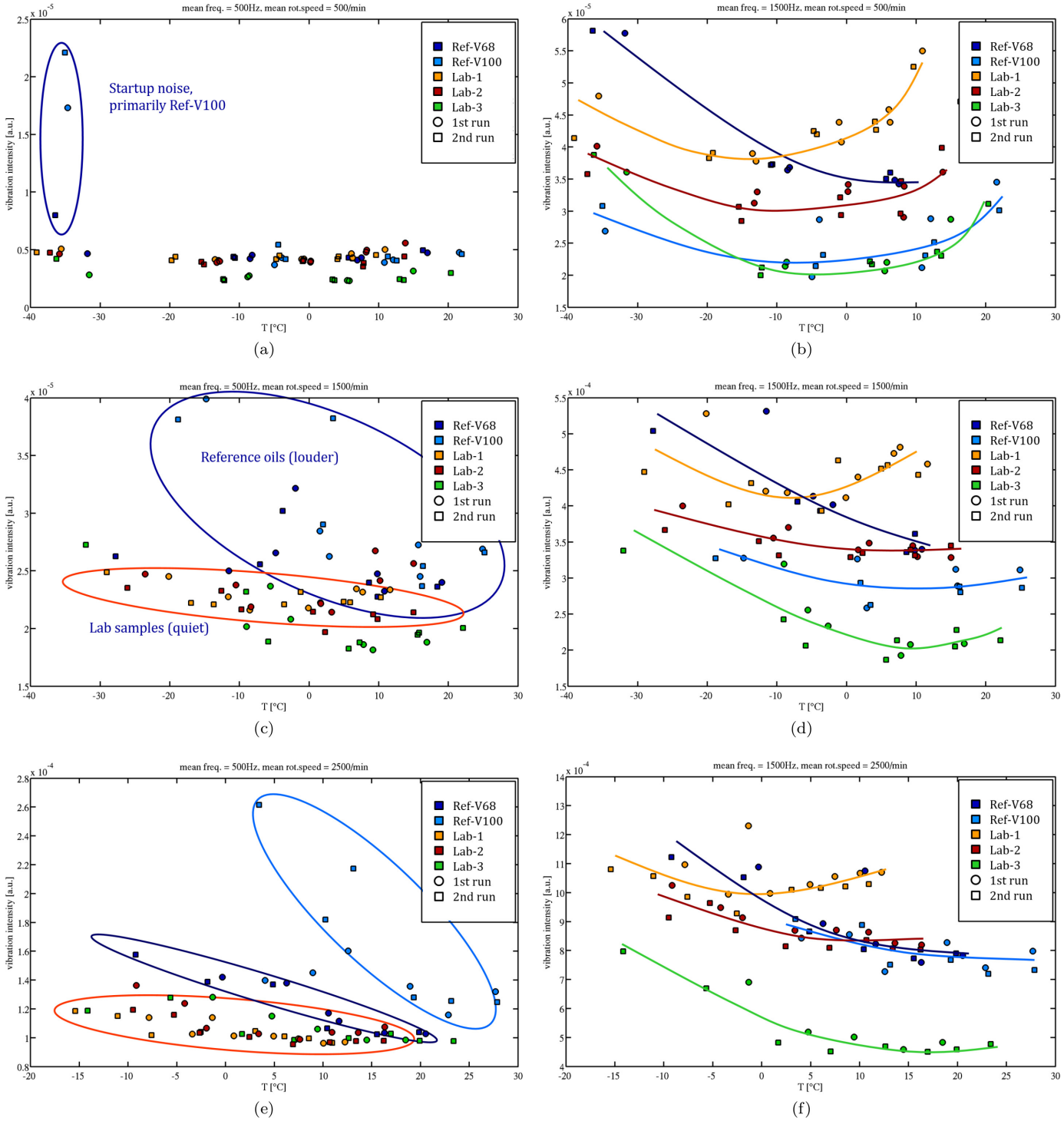

Figure 10: Comparison of the temperature dependence of the vibration intensity for all five tested oils. Left column: lower frequency band (0–1000 Hz), right column: upper frequency band (1000–2000 Hz). Mean rotational speed 500 min^{-1} (top), 1500 min^{-1} (mid), 2500 min^{-1} (bottom). Annotated ellipses and curves merely guide the eye.

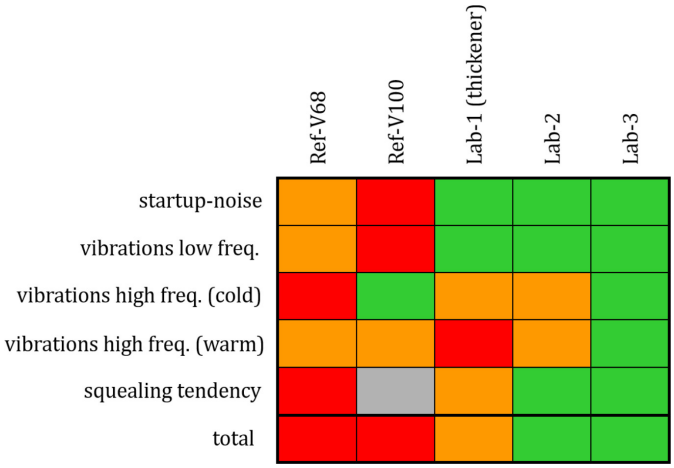

Figure 11: Ranking matrix comparing the five tested lubricants according to five criteria.

[3] Nic Veloff, Anil Nadkarni, and Thomas Murphy. Better performance for self-lubricating bronze bearings. *Metal Powder Report*, 61(8):31–41, 2006.

[4] Ertuğrul Durak. Experimental investigation of porous bearings under different lubricant and lubricating conditions. *KSME International Journal*, 17(9):1276–1286, Sep 2003.

[5] A Krol, B Giemza, and T Kaldonski. The failure of an electric engine caused by the seizure of the porous bearing. In *ASME/STLE 2007 International Joint Tribology Conference*, pages 447–449. American Society of Mechanical Engineers, 2007.

[6] Bolesław Giemza, Tadeusz Kałdoński, and Artur Król. Problem of the service life of self-lubricated friction couples. In *Mechatronic Systems and Materials*, volume 113 of *Solid State Phenomena*, pages 399–404. Trans Tech Publications, 7 2006.

[7] Teruo Shimizu and Teruhisa Watanabe. Effects of lubricating oil on the sliding noise of sintered porous bearings of bronze. *Journal of the Japan Society of Powder and Powder Metallurgy*, 28(4):131–135, 1981.

[8] SK Rhee, PHS Tsang, and YS Wang. Friction-induced noise and vibration of disc brakes. *Wear*, 133(1):39–45, 1989.

[9] Frank Chen, H Tong, SE Chen, and R Quaglia. On automotive disc brake squeal part iv reduction and prevention. Technical report, SAE Technical Paper, 2003.

[10] Frank Chen. Automotive disk brake squeal: an overview. *International Journal of Vehicle Design*, 51(1-2):39–72, 2009.

[11] Eckhard Kirchner, Klaus Hartmut Köster, Frank Langer, Andreas Nicola, and Bernd Sauer. Model-based analysis of the "cold start squeal" phenomenon of clutches. *ATZ worldwide*, 107(9):38–40, 2005.

[12] Paul J Shayler, Warren S Baylis, and Michael Murphy. Main bearing friction and thermal interaction during the early seconds of cold engine operation. In *ASME 2002 Internal Combustion Engine Division Fall Technical Conference*, pages 445–459. American Society of Mechanical Engineers, 2002.

[13] RA Ibrahim. Friction-induced vibration, chatter, squeal, and chaos—part i: Mechanics of contact and friction. *Applied Mechanics Reviews*, 47(7):209–226, 1994.

[14] Adnan Akay. Acoustics of friction. *The Journal of the Acoustical Society of America*, 111(4):1525–1548, 2002.

[15] Ioana Adina Neacşu, Bernhard Scheichl, Georg Vorlaufer, Stefan J Eder, Friedrich Franek, and Lutz Ramonat. Experimental validation of the simulated steady-state behavior of porous journal bearings. *Journal of Tribology*, 138(3):031703, 2016.

[16] F Dalzin, A Le Bot, J Perret-Liaudet, and D Mazuyer. Tribological origin of squeal noise in lubricated elastomer–glass contact. *Journal of Sound and Vibration*, 372:211–222, 2016.

[17] Shie Qian and Dapang Chen. Joint time-frequency analysis. *IEEE Signal Processing Magazine*, 16(2):52–67, 1999.

[18] Andrzej Majkowski, Marcin Kołodziej, and Remigiusz J Rak. Joint time-frequency and wavelet analysis-an introduction. *Metrology and Measurement Systems*, 21(4):741–758, 2014.

[19] R Vio and W Wamsteker. Joint time–frequency analysis: A tool for exploratory analysis and filtering of non-stationary time series. *Astronomy & Astrophysics*, 388(3):1124–1138, 2002.

[20] Leon Cohen. *Time-frequency analysis*, volume 778. Prentice Hall PTR Englewood Cliffs, NJ:, 1995.